

## Polymer-Stabilized Gold Nanoparticles and Their Incorporation into Polymer Matrices

Muriel K. Corbierre,<sup>†</sup> Neil S. Cameron,<sup>†</sup> Mark Sutton,<sup>‡</sup>  
Simon G. J. Mochrie,<sup>§</sup> Laurence B. Lurio,<sup>||</sup> Adrian Rühm,<sup>||</sup> and  
R. Bruce Lennox<sup>\*,†</sup>

Departments of Chemistry and Physics  
McGill University, 801 Sherbrooke Street West  
Montréal, H3A 2K6 Québec

Departments of Physics and Applied Physics  
Yale University, New Haven, Connecticut 06520  
Center for Materials Science and Engineering  
Massachusetts Institute of Technology  
Cambridge, Massachusetts 02139-4307

Received July 16, 2001

Functionalized metal nanoparticles are of great interest in terms of their potential applications in biomedical, electronic, and optical materials.<sup>1</sup> Such systems have been extensively studied over the past decade following synthetic advances.<sup>2</sup> Incorporation of nanoparticles in polymer matrices is a field of particular interest for materials engineering and the study of nanoparticle–matrix interactions.<sup>3</sup> Although there are many examples of ligand-stabilization of nanoparticles, there are few examples of polymer-stabilized metal nanoparticles where the polymer is linear and has one well-defined point of attachment.<sup>4</sup>

There have been a variety of attempts to achieve nanoparticle–polymer composites. Overall, we note two different approaches used to date. The first technique consists of the in situ preparation of the nanoparticles in the matrix. This is effected either by the reduction of metal salts dissolved in the polymer matrix<sup>5</sup> or by the evaporation of metals on the heated polymer surface.<sup>6</sup> A second, less common technique, involves polymerizing the matrix around the nanoparticles.<sup>7</sup> A desirable approach would involve the blending of *pre-made* nanoparticles into *pre-synthesized* polymer. This provides full synthetic control over both the nanoparticles and the matrix, and has the potential for generating a wide variety of composite materials. Preliminary work in our laboratory with alkanethiol-decorated gold nanoparticles demonstrated difficulty in dispersing these nanoparticles into a variety of polymer matrices, such as polystyrene (PS) and poly(dimethylsiloxane) (PDMS). Gold nanoparticle aggregates were always

formed in the polymer matrices, with dimensions on the order of several hundreds of nanometers.<sup>8</sup>

To overcome these difficulties, we reasoned that it is necessary to design the coating of the nanoparticles to make them compatible with the polymer matrix. We speculated that gold nanoparticles whose polymer ligand is chemically the same as the matrix would be more thermodynamically favorable to their incorporation.<sup>9</sup> In this communication we describe the synthesis of novel gold nanoparticles (PS–Au) decorated with covalently bound thiol-capped polystyrene macromolecules (PS–SH), and their successful dispersion in a PS matrix. Polystyrene was chosen because its high glass-transition temperature ( $T_g \approx 100$  °C) allows for the formation of robust films at room temperature. The PS–SH macromolecules were synthesized by anionic polymerization.<sup>10</sup> The polystyrene anion was titrated with one unit of propylene sulfide to generate the thiol end group. The presence of the thiol end group was confirmed by <sup>13</sup>C NMR. Gel permeation chromatography (GPC) provided the number average molecular weight and the polydispersity index ( $M_n$  13 300 g/mol, PI 1.7).

The PS–Au nanoparticles were prepared following modified Ulman reaction conditions,<sup>11</sup> using a 1/3.5 thiol/HAuCl<sub>4</sub> reagent ratio and lithium triethylborohydride (Superhydride, Aldrich) as the reducing agent. UV–vis spectroscopy of a PS–Au solution in toluene confirmed the presence of the plasmon band at 523 nm, which is in the region characteristic of alkanethiol-capped gold nanoparticles.<sup>12</sup> The nanoparticles were isolated and redissolved several times in solvents (e.g., chloroform) that are also solvents for the PS ligand. The Au core diameters were determined from transmission electron micrographs (TEM) and exhibit a moderate degree of polydispersity ( $6.2 \pm 1.7$  nm). Most of the nanoparticles appear to be spherically symmetric. However, several of the larger nanoparticles appear to be not particularly spherical.

Incorporation of PS–Au into the PS matrix ( $M_n$  46 400 g/mol, PI 1.05) was effected using chloroform as solvent. Both PS–Au and PS were dissolved in a small amount of chloroform and gently stirred for a few hours until the solution appeared homogeneously colored (purple). A 1.5 mm × 0.1 mm Nichrome ribbon, bent into the shape of a loop (~2 mm diameter), was dipped several times into a viscous PS–Au/PS chloroform solution (0.1%  $V_{Au}/V_{PSmatrix}$ ). Sufficient time (~20 min) elapsed between dips to allow most of the solvent to evaporate at room temperature. Several days at ambient temperature elapsed before the samples were sectioned (diamond knife). Sectioning provided samples of  $75 \pm 15$  nm in thickness for TEM observation. The electron-dense gold core of the PS–Au colloids allowed for high contrast even in thick-sectioned samples. A remarkably even dispersion of the PS–Au colloids in the PS matrix was observed, with an average edge-to-edge distance between the colloids of 60 nm<sup>13</sup> (Figure 1A). The volume fraction of the initial solution is 0.001, and the volume fraction of gold cores in the PS matrix observed in TEM is ca. 0.001.

\* Author for correspondence. E-mail: bruce.lennox@mcgill.ca.

<sup>†</sup> Department of Chemistry, McGill University.

<sup>‡</sup> Department of Physics, McGill University.

<sup>§</sup> Departments of Physics and Applied Physics, Yale University.

<sup>||</sup> Center for Materials Science and Engineering, MIT.

(1) See for example: (a) Storhoff, J. J.; Elghanian, R.; Mucic, R. C.; Mirkin, C. A.; Letsinger, R. L. *J. Am. Chem. Soc.* **1998**, *120*, 1959–1964. (b) Wohltjen, H.; Snow, A. W. *Anal. Chem.* **1998**, *70*, 2856–2859. (c) Demaille, C.; Brust, M.; Tsiouky, M.; Bard, A. J. *Anal. Chem.* **1997**, *69*, 2323–2328.

(2) (a) Brust, M.; Walker, M.; Bethell, D.; Schiffrin, D. J.; Whyman, R. J. *Chem. Soc., Chem. Commun.* **1994**, 801–802. (b) Hostetler, M. J.; Templeton, A. C.; Murray, R. W. *Langmuir* **1999**, *15*, 3782–3789.

(3) (a) Ziolo, R. F.; Giannelis, E. P.; Weinstein, B. A.; O'Horo, M. P.; Ganguly, B. N.; Mehrotra, V.; Russell, M. W.; Huffman, D. R. *Science* **1992**, *257*, 219–223. (b) Becroft, L. L.; Ober, C. K. *Chem. Mater.* **1997**, *9*, 1302–1317.

(4) (a) Wuelfing, W. P.; Gross, S. M.; Miles, D. T.; Murray, R. W. *J. Am. Chem. Soc.* **1998**, *120*, 12696–12697. (b) Teranishi, T.; Kiyokawa, I.; Miyake, M. *Adv. Mater.* **1998**, *10*, 596–599. (c) Teranishi, T.; Hosoe, M.; Miyake, M. *Adv. Mater.* **1997**, *9*, 65–67. (d) Jordan, R. West, N.; Ulman, A.; Chou, Y.-M.; Nuyken, O. *Macromolecules* **1999**, *34*, 1606–1611.

(5) (a) Mayer, A. B. R. *Mater. Sci. Eng.* **1998**, *C6*, 155–166. (b) Selvan, S. T.; Spatz, J. P.; Klok, H.-A.; Möller, M. *Adv. Mater.* **1998**, *10*, 132–134. (c) Watkins, J. J.; McCarthy, T. J. *Chem. Mater.* **1995**, *7*, 1991–1994.

(6) Sayo, K.; Deki, S.; Hayashi, S. *Eur. Phys. J. D* **1999**, *9*, 429–432.

(7) Lee, J.; Sundar, V. C.; Heine, J. R.; Bawendi, M. G.; Jensen, K. F. *Adv. Mater.* **2000**, *12*, 1102–1105.

(8) Unpublished results: M.K.C., N.S.C., R.B.L.

(9) Cowie, J. M. G. *Polymers: Chemistry and Physics of Modern Materials*, 2nd ed.; Blackie Academic & Professional: New York, 1991.

(10) Stouffer, J. M.; McCarthy, T. J. *Macromolecules* **1988**, *21*, 1204–1208.

(11) Yee, C. K.; Jordan, R.; Ulman, A.; White, H.; King, A.; Rafailovich, M.; Sokolov, J. *Langmuir* **1999**, *15*, 3486–3491.

(12) Hostetler, M. J.; Wingate, J. E.; Zhong, C.-J.; Harris, J. E.; Vachet, R. W.; Clark, M. R.; Londono, J. D.; Green, S. J.; Stokes, J. J.; Wignall, G. D.; Glush, G. L.; Porter, M. D.; Evans, N. D.; Murray, R. W. *Langmuir* **1998**, *14*, 17–30.

(13) Due to the thickness of the sectioned samples (between 60 and 85 nm), it is difficult to precisely measure the distance between particles in a 2D plane; thus, the average distance can only be estimated. A simple geometrical treatment leads to the conclusion that an “apparent” distance of 60 nm between 2 colloids in a *x*–*y* plane can in fact be 96 nm if one colloid is situated 75 nm “deeper” in the *z*-axis of the plane.

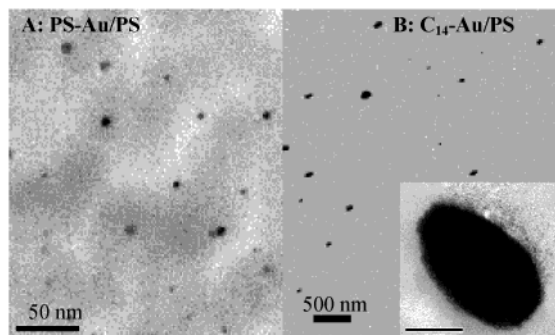


**Figure 1.** (A, B) TEM images of sectioned sections of (A) PS-Au nanoparticles in a PS matrix, (B)  $C_{14}$ -Au aggregates in a PS matrix. Inset: aggregate enlargement, scale bar = 100 nm.

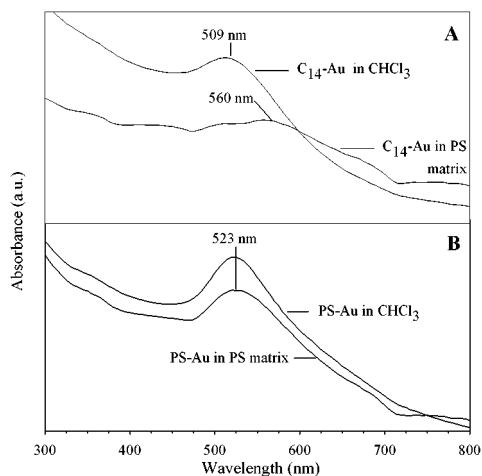


**Figure 2.** UV/vis absorption spectra of (A)  $C_{14}$ -Au and  $C_{14}$ -Au/PS; (B) PS-Au and PS-Au/PS.

Tetradecanethiol-Au colloids ( $C_{14}$ -Au), prepared by the Ulman-type reaction ( $3.2 \pm 0.4$  nm in diameter), were also incorporated into PS ( $M_n$  57 000 g/mol, PI 2.0) and PDMS (5000 cS, United Chemical Technologies) matrices. The  $C_{14}$ -Au/PS samples were sectioned and analyzed by TEM. Unlike the PS-capped material, the Au- $C_{14}$  nanoparticles in the PS matrix assembled into aggregates of several tens of nanometers in diameter (Figure 1B).

UV-vis spectroscopy was used to characterize both the PS-Au/PS and the  $C_{14}$ -Au/PS ( $M_n$  46 400 g/mol, PI 1.05) composites. The UV-vis spectrum of a gold nanoparticle sample is a very sensitive reporter of particle aggregation state.<sup>14</sup> UV-vis spectra of PS-Au and  $C_{14}$ -Au in  $CHCl_3$  (300–800 nm) exhibit maxima attributable to a plasmon resonance. These maxima in  $CHCl_3$  are 523 and 509 nm for PS-Au and  $C_{14}$ -Au, respectively (Figure 2). Films of PS-Au/PS and  $C_{14}$ -Au/PS (0.1%  $V_{Au}/V_{PS}$  matrix) were drop-cast from  $CHCl_3$  solution inside quartz cuvettes and allowed to dry slowly in a near-saturated atmosphere for several days. The plasmon band resonance of the PS-Au/PS sample is 523 nm (Figure 2B) but for  $C_{14}$ -Au/PS it is both broadened and shifted to 560 nm (Figure 2A). In the latter case, single nanoparticles are still present in the UV-vis film, and the sample is purple-blue. This is due to a trapping of the  $C_{14}$ -Au in the single particle state caused by rapid evaporation of the solvent. A similar trapping phenomenon of CdS colloids has been reported by Fogg et al.<sup>15</sup>

The incorporation of the PS-Au nanoparticles in the 46 kD PS matrix resulted in a uniform dispersion of the PS-Au

throughout the sample (Figure 1A). The absence of aggregates<sup>16</sup> is significant given that the incorporation of  $C_{14}$ -Au nanoparticles into PDMS and PS matrices leads to intractable aggregation. In the latter case, TEM images of sectioned samples of  $C_{14}$ -Au nanoparticles in the 57 kD PS sample indicated the formation of regular aggregates on the order of several hundreds of nanometers in diameter (Figure 1B). A study by Dirix et al.<sup>17</sup> which involved blending  $C_{12}$ -Au nanoparticles into high-density polyethylene (using *p*-xylene as a solvent and heating to 130 °C) also led to the formation of aggregates. In this case the desorption of the thiols from the Au at such a high temperature was the probable cause of aggregation.

We observed that nanoparticle aggregation is readily visualized in the  $C_{14}$ -Au/PS and  $C_{14}$ -Au/PDMS samples, where they pass from pink to blue upon slow removal of the solvent. The color of the gold nanoparticle solution is a sensitive function of the position of the surface plasmon band resonance (usually around 510–520 nm), depending on several factors including particle size, surface functionality, solvent, and temperature.<sup>12,18</sup> Moreover, when gold nanoparticles are brought into close contact with one another, plasmon resonance coupling of the colloids results in both a red-shift of the plasmon band and an increase in the Rayleigh scattering.<sup>14,19</sup> This wavelength shift appears in the UV-vis spectra of the  $C_{14}$ -Au/PS system (Figure 2A). The PS-Au/PS system, however, does not show any plasmon absorbance coupling (Figure 2B). This confirms the absence of aggregates or even particle pairs whose edge-to-edge distances are less than 8 nm.<sup>20</sup>

Small-angle X-ray scattering (SAXS) has been used in preliminary measurements to determine the state of the nanoparticles. Aggregates are detected in the  $C_{14}$ -Au/PS system whereas individual particles are detected in the PS-Au/PS system. SAXS is a powerful tool for the study of these systems since it allows for in situ observation.<sup>21</sup>

This study is significant for several reasons. (1) We report the first successful blending of *pre-made* Au nanoparticles into *pre-synthesized* polymer matrices, where the particles are thoroughly dispersed in the matrix. (2) The principal advantage of this method resides in the synthetic control possible over both the nanoparticles and the matrix, as opposed to the in situ preparations currently found in the literature. (3) The simplicity of this method makes it very appealing, since it involves only the use of a compatible, volatile solvent and a film support. (4) This strategy should be generally applicable to other systems, due to the availability of a number a different thiol-capping agents and polymers. Tuning of the Au nanoparticle coating so that it is compatible with the matrix of choice will thus be realizable.

**Acknowledgment.** We thank Ms. J. Mui for sectioning the TEM samples and Professor D. Patterson for helpful discussions. NSERC (Canada) provided funding of this research. S.M. is supported by NSF DMR 0071755.

JA0166287

(15) See for example: Fogg, D. E.; Radzilowski, L. H.; Dabbousi, B. O.; Schrock, R. R.; Thomas, E. L.; Bawendi, M. G. *Macromolecules* **1997**, *30*, 8433–8439.

(16) The equivalent of 300 TEM images were thoroughly analyzed.

(17) Dirix, Y.; Darribère, C.; Heffels, W.; Bastiaansen, C.; Caseri, W.; Smith, P. *Appl. Opt.* **1999**, *38*, 6581–6586.

(18) Link, S.; El-Sayed, M. A. *J. Phys. Chem. B* **1999**, *103*, 4212–4217.

(b) Shipway, A. N.; Katz, E.; Willner, I. *ChemPhysChem* **2000**, *1*, 18–52.

(19) Shipway, A. N.; Lahav, M.; Gabai, R.; Willner, I. *Langmuir* **2000**, *16*, 8789–8795.

(20) Storhoff, J. J.; Lazarides, A. A.; Mucic, R. C.; Mirkin, C. A.; Letsinger, R. L.; Schatz, G. C. *J. Am. Chem. Soc.* **2000**, *122*, 4640–4650.

(21) TEM, on the other hand, always has the potential to be problematic, given that sample preparation/treatment and beam conditions might alter the gold nanoparticles and even provoke the formation of aggregates.

(14) Kim, Y.; Johnson, R. C.; Hupp, J. T. *Nano Lett.* **2001**, *1*, 165–167.